JOURNAL OF MATERIALS SCIENCE 32 (1997) 451–457

The compressive behaviour of porous copper made by the GASAR process

A. E. SIMONE, L. J. GIBSON
Department of Civil and Environmental Engineering, Massachusetts Institute of Technology, Cambridge, MA 02139, USA

Recently, porous metals and ceramics have been made by melting the solid in a hydrogen atmosphere and then cooling through the eutectic point; the technique is known as the GASAR process. The size, shape, orientation and volume fraction of the pores can be controlled by the direction and rate of cooling and the pressure of the system. Here we describe the uniaxial compressive behaviour of GASAR copper with cylindrical pores oriented in the direction of loading. The elastic modulus and yield strength of the porous materials increase linearly with increasing relative density. Initial plastic deformation was found to be due to plastic yielding of the solid rather than buckling of the cells walls. The characteristic densification strain decreased linearly with increasing relative density.

1. Introduction

Porous metals can be made by melting the solid in an atmosphere of hydrogen and then cooling through the eutectic point. The GASAR process, developed at the Dnepropetrovsk Metallurgical Institute (DMI) in Ukraine, is compatible with a wide variety of pure metals, such as copper, aluminium and nickel, as well as alloys, such as steel and bronze. Relative densities between 0.25 and 0.95 and pores sizes between 10 μm and 5 mm can be produced by control of the pressure of the hydrogen atmosphere and the solidification rate. A variety of pore structures can be produced by controlling the pressure, the cooling rate and the direction of the applied temperature gradient during solidification; for instance, longitudinal or radial pores can be created by cooling from the bottom or the sides of a cylindrical mould. Layered structures, with alternating bands of solid and porous material, are also possible. The process is described in more detail by Simone and Gibson [1], who studied the tensile behaviour of porous GASAR copper specimens with elongated cylindrical pores oriented in the direction of testing. Here we describe the compressive behaviour of GASAR copper specimens with cylindrical pores again oriented in the loading direction.

2. Experimental procedure

2.1. Materials

Thirty cylindrical porous GASAR copper specimens, 50 mm diameter and 100 mm high, with relative densities from 0.35–0.70 and pore diameters from 2–5 mm, were obtained from DMI through USP Holdings (Ann Arbor, MI). Nominally solid cast copper ingots of the same size were also obtained.

2.2. Microstructural examination

Transverse and longitudinal sections of selected specimens ($\rho^*/\rho_s = 0.609, 0.556, 0.494, 0.456, 0.384, 0.375$) were cut using either a Struers (Westlake, OH) Discotom cut-off saw or an EDM Technology (Long Island, NY) 2000B electric discharge machine for examination of the pore and grain structure. A transverse cross-sectional cut was made near one end of each untested specimen, and the remaining specimen was then bisected longitudinally. The transverse cross-section and one longitudinal section of each specimen were then ground and polished on a Buehler Ltd (Metals Park, OH) polishing wheel using silicon carbide papers and 1.0 and 0.05 μm alumina micropolish. The longitudinal sections were coated with spray graphite before polishing in order to add contrast and reduce reflective glare from the interior pore surface in later photography. A light etch was applied to the polished surfaces using a solution of 3 g $FeCl_3$, 10 ml HCl and 100 ml H_2O [3] in order to reduce glare. This was followed by the application of a thin layer of petroleum jelly to prevent surface corrosion. Photos of these prepared sections were taken with a Polaroid (Cambridge, MA) MP-4 Land Camera.

The remaining longitudinal section of each specimen was used for examination of the grain structure. Because the pore structure of the GASAR ingots was found to be inhomogeneous, with significant end effects, the transverse grain structure of each ingot was examined from a section cut at least 3 cm from the end of this remaining section. This transverse section and the remaining longitudinal section were then ground and polished using the procedure described above. Transverse and longitudinal sections of the solid copper ingots were also prepared. The polished faces were then macroetched using a solution of 50 ml HNO_3

0022–2461

and 50 ml H_2O [4] and microetched using a solution of 5 g $FeCl_3$, 50 ml HCl and 100 ml H_2O [3] to show grain boundaries. Polaroid photos of these sections were also taken. Selected photos were digitized and enhanced using a scanner and NIH Image v.1.58 on a Macintosh computer. Edge detection filters and intensity thresholding were used to form a sharp binary image.

Pore and grain size measurements were made on each untested specimen in both the transverse and longitudinal directions. The average size and standard deviation of size were computed based on measurements made directly from the specimens and photographs. Each computed value is based on 30–50 individual measurements.

2.3. Compression testing

Compression tests were performed on the full length of the ingot after the ends were milled on a Bridgeport machine to ensure that they were plane and parallel. The diameter of each specimen was at least 12 times as large as the mean pore size in the transverse direction.

The specimens were first loaded in compression using displacement control on an Instron (Canton, MA) model 8500 load frame with a 100 kN load cell. The strain was measured using an Instron cantilever-arm extensometer (model 2620–826) with a 50 mm gauge length and a range of 5% strain. The load and strain were recorded using a Hewlett–Packard (Palo Alto, CA) Data Acquisition/Control Unit (3497A) and a personal computer. The Young's modulus and 0.002 offset yield strength were then measured using linear regression and graphical analysis of the stress–strain curve. Specimens were tested to a maximum strain of 0.02 and were then unloaded. The actuator speed during each test was 1.66×10^{-3} mm s^{-1}, corresponding to a strain rate of approximately 1.66×10^{-5} s^{-1}.

Once the Young's modulus and yield strength were determined, the specimens were reloaded on a Baldwin (company now defunct) 880 kN capacity hydraulic load frame to a maximum load of approximately 800 kN in order to investigate the plastic collapse and densification behaviour. The actuator speed during these tests was 6.67×10^{-2} mm s^{-1}, corresponding to a strain rate of approximately 6.67×10^{-4} s^{-1}. Crosshead deflection was measured with a Celesco (Canoga Park, CA) DPT250 displacement transducer. The load and crosshead deflection were recorded by an Advanced Machine Technology, Inc. (Cambridge, MA) signal acquisition and control system running on a personal computer. In the large deflection tests, the strain was defined as the ratio of crosshead deflection to the original specimen height. Selected specimens were loaded to 10% or 30% strain and then unloaded for later examination of the plastic deformation. After testing, the specimens were cut longitudinally and the pore structure photographed using the methods described for microstructural analysis of the untested specimens.

3. Results

3.1. Microstructural analysis

Longitudinal and transverse sections of untested porous GASAR specimens are shown in Fig. 1. The pore structure is inhomogeneous: the size, shape and orientation of the pores vary with longitudinal position within each specimen and also from one specimen to the next. Significant end effects are also evident in most samples, indicating that a uniform directional temperature gradient could not be maintained during processing. The data for the pore size and grain size measurements are listed in Table I.

At relative densities greater than 0.5, the pores are roughly parallel to the longitudinal direction, but are highly segmented and discontinuous, possibly as a result of the control conditions during directional solidification. The aspect ratio of the pores varies from about 1.5–8, with an average between 3 and 5. At relative densities less than 0.5, the GASAR specimens are more homogeneous: the pores are more closely oriented in the longitudinal direction and there are fewer discontinuities present. The aspect ratio of these pores is typically between 8 and 12.

The grain structure of typical GASAR specimens in the transverse and longitudinal directions is shown in Fig. 2. At higher relative densities the grains are highly irregular in shape, have an aspect ratio of 3–4, and are only roughly oriented in the longitudinal direction, while at lower relative densities, the grains are more regular, have an average aspect ratio of approximately 7–15, and are strongly oriented in the longitudinal direction. The transverse grain size does not appear to be dependent on porosity. All specimens show an average transverse grain size of approximately 1–2.5 mm.

The solid ingots have a radially oriented columnar grain structure, which we take to be the result of a radial cooling gradient during solidification. This grain structure is entirely different from that of the porous GASAR specimens which were cooled longitudinally. The size and aspect ratio of the grains in the solid ingots is roughly comparable to that of the porous GASAR specimens.

3.2. Compression testing

Typical stress–strain curves for the porous GASAR specimens are shown in Fig. 3 for three relative densities. The curves show that as relative density decreases, the Young's modulus, the yield strength and the slope of the stress–strain curve through the plastic collapse region all decrease, while the strain at which densification begins increases. Material non-uniformity caused significant distortion of many specimens during plastic collapse. Fig. 4 shows photographs of longitudinal sections of two specimens compressed to 30% strain. Diagonal bands of localized buckling appeared on many specimens, particularly those with lower relative density. Specimens compressed to 10% strain showed little, if any, cell-wall buckling.

The Young's modulus and 0.002 offset strain yield strength data are plotted against relative density in Figs 5 and 6, respectively. Data for the nominally solid

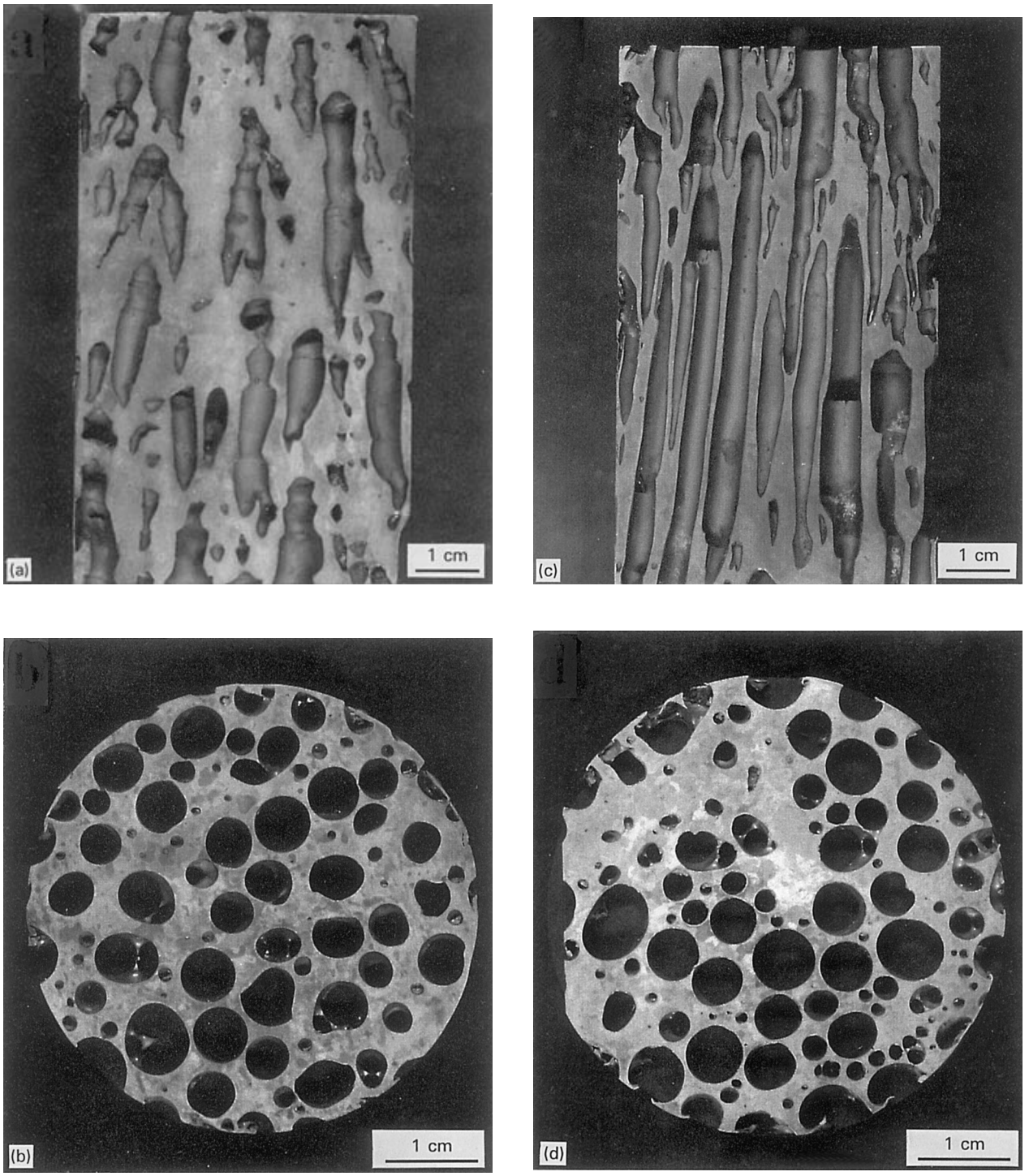

Figure 1 Photographs of longitudinal (a, c) and transverse (b, d) cross-sections of porous GASAR copper: (a, b) $\rho^*/\rho_s = 0.61$ (c, d) $\rho^*/\rho_s = 0.38$.

copper with radially oriented columnar grains are also plotted, as are the tensile data for nominally solid copper with longitudinal grains obtained from DMI [1]. The modulus and yield strength of the porous GASAR specimens increase linearly with relative density. The solid lines in Figs 5 and 6 represent the linear regressions

$$E^* = -16.8 + 94.1\left(\frac{\rho^*}{\rho_s}\right) \qquad (r^2 = 0.539) \quad (1)$$

and

$$\sigma^*_{YS} = 2.1 + 21.2\left(\frac{\rho^*}{\rho_s}\right) \qquad (r^2 = 0.624) \quad (2)$$

respectively.

Because the transition from plastic collapse to densification is not well defined in the higher relative density specimens, it is difficult to establish a consistent criterion for measuring the densification strain over the entire range of specimen porosities. In order to make a comparative measure of the densification behaviour, the stress-strain curve of each specimen was normalized by its measured yield strength. The yield strength is a reasonable normalization factor in this case because both the yield strength and densification strain are linearly dependent on porosity [5]. Typical normalized stress–strain curves are shown in Fig. 7. For each specimen, the strain corresponding to a normalized stress of $\sigma^*/\sigma^*_{YS} = 25$ was recorded. This value was chosen because it is the maximum

TABLE I Pore-size and grain-size measurements for selected specimens (standard deviation in parentheses)

Relative density, ρ^*/ρ_s	Transverse pore size, ϕ (mm)	Axial pore size (mm)	Transverse grain size, d (mm)	Axial grain size (mm)
0.609	3.71 (1.83)	16.83 (11.28)	2.27 (0.85)	7.74 (4.59)
0.556	3.11 (1.79)	13.90 (11.42)	2.29 (1.03)	7.21 (4.35)
0.494	2.36 (1.10)	29.43 (25.77)	1.89 (0.85)	20.66 (16.16)
0.456	3.76 (1.58)	38.01 (27.34)	1.97 (0.81)	15.73 (7.78)
0.384	1.77 (0.78)	24.32 (9.75)	1.10 (0.59)	16.38 (8.68)
0.375	2.91 (1.42)	25.12 (23.80)	1.72 (0.92)	15.11 (5.26)

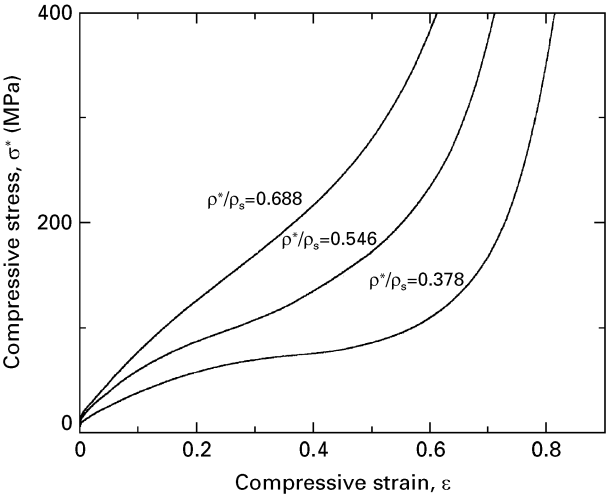

Figure 3 Typical compressive stress–strain curves.

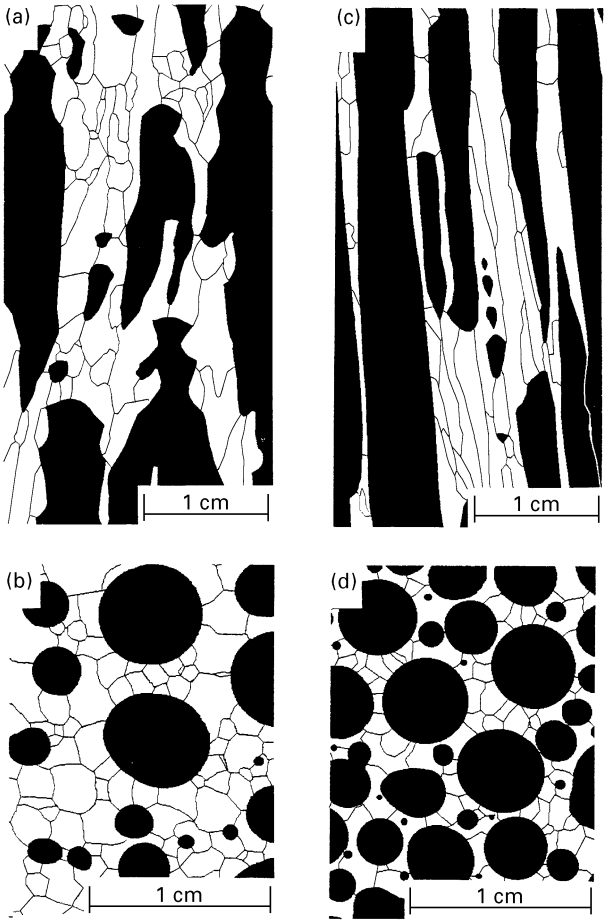

Figure 2 Digitally enhanced photographs showing the longitudinal and transverse grain structure. (a, b) $\rho^*/\rho_s = 0.61$ (c, d) $\rho^*/\rho_s = 0.38$.

normalized stress that could be imparted on all specimens on the load frame used for the tests. The densification strain is plotted against porosity in Fig. 8. The solid line represents the linear regression of these data

$$\varepsilon_D = 0.905 - 0.432\left(\frac{\rho^*}{\rho_s}\right) \qquad (r^2 = 0.870) \quad (3)$$

4. Discussion

In porous GASAR copper with a 30–200 μm pore size, the grain and pore structures have been shown to be

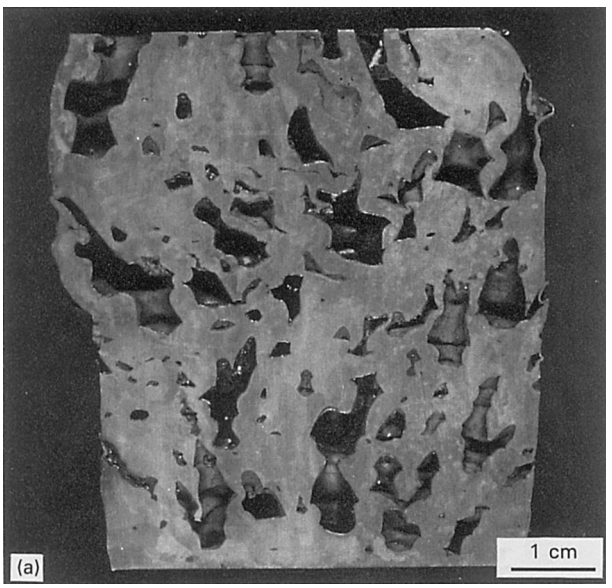

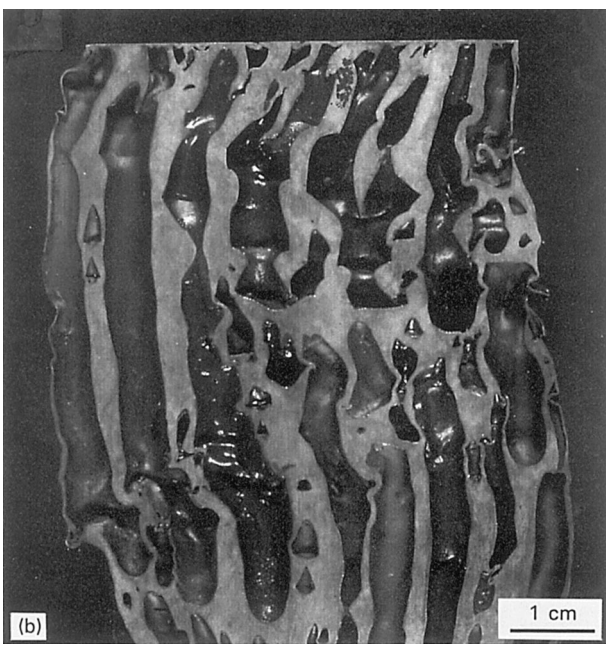

Figure 4 Photographs of longitudinal cross-sections of specimens compressed to 30% strain. (a) $\rho^*/\rho_s = 0.58$ (b) $\rho^*/\rho_s = 0.37$.

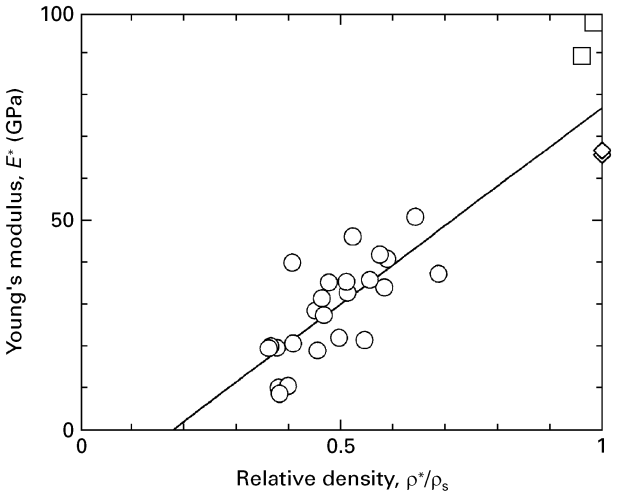

Figure 5 Young's modulus plotted against relative density. (○) Compression, porous GASAR; (□) compression, radial grains; (◇) tension, longitudinal grains [1].

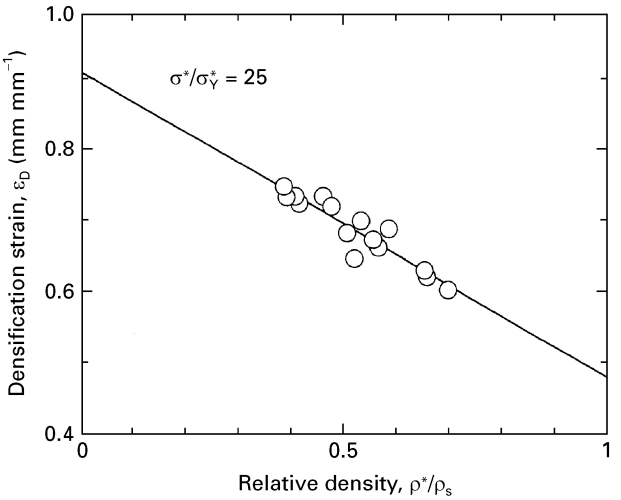

Figure 8 Densification strain, measured at $\sigma^*/\sigma_{Ys}^* = 25$, plotted against relative density.

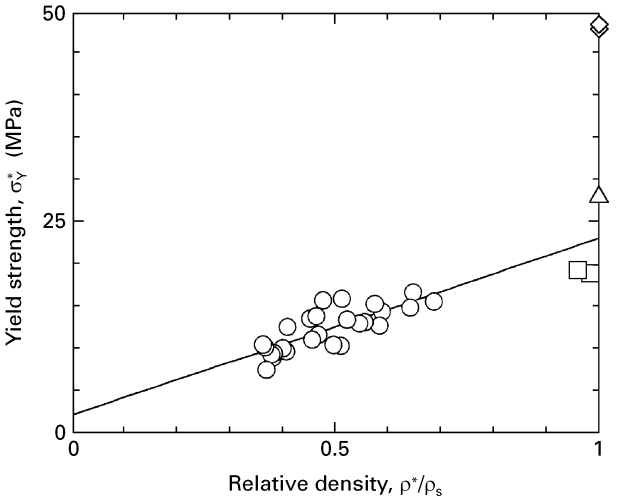

Figure 6 Yield strength in compression plotted against relative density. All measurements used a 0.002 offset strain except (△) compression, equiaxed grains [7], which used a 0.005 offset strain. (◇) Tension, longitudinal grains [1], (○) compression, porous GASAR; (□) compression, radial grains.

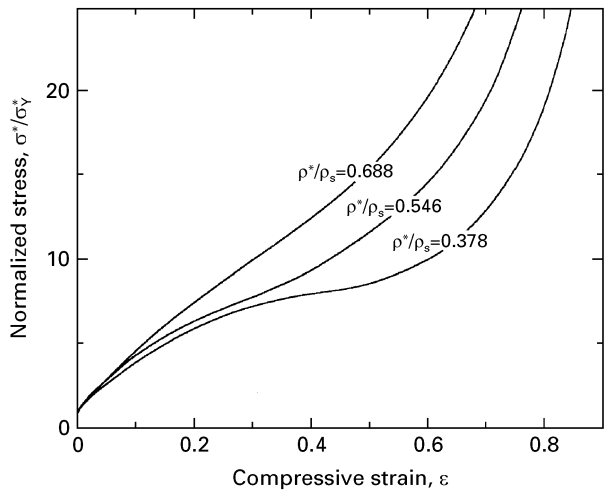

Figure 7 Normalized compressive stress, σ^*/σ_{Ys}^*, plotted against strain.

very similar in terms of orientation and aspect ratio [1]. From Fig. 2 and the data in Table I, it can be seen that the 2–5 mm pore size GASAR specimens also exhibit such a similarity. As the relative density decreases, both the pores and the grains become more strongly oriented in the longitudinal direction, and the aspect ratio of each increases.

The roughly linear dependence of Young's modulus and yield strength on porosity is consistent with the expected behaviour of a material with cylindrical pores oriented in the loading direction [1, 5]. The high degree of scatter in the measured data can be attributed to the inhomogeneous pore structure of the specimens. The intercepts of the linear regressions are expected to correspond to the measured properties of the solid ingots. The discrepancies between these two values can be at least partially explained by the difference in grain structure between the solid and porous specimens. The elastic and yield properties of face-centred cubic (fcc) materials like copper are highly sensitive to crystallographic orientation [6]. Copper with a random crystallographic orientation typically has a Young's modulus of 110 MPa [7]. Copper with a ⟨1 0 0⟩ preferred orientation, typical of directionally solidified fcc materials, has a modulus of about 67 MPa [8]. The intercept Young's modulus of 77.3 MPa is consistent with a material with a roughly ⟨1 0 0⟩ crystallographic texture, as expected. The intercept yield strength of 23.2 MPa is comparable to the measured yield strength of the solid ingot and to the ASM Metals Handbook value of cast copper yield strength. It should be noted that the yield strength of a columnar grain structure decreases slightly when tested in a direction normal to the plane of grain orientation [9].

The compressive yield strength values reported here for both the solid and porous copper materials are significantly lower than the tensile yield strength values reported by Simone and Gibson [1]. In terms of material structure, the specimens used in this study had a significantly lower level of microstructural consistency, and both the pore size and grain size are considerably larger. The relationship of the grain

structure to the pore structure is also different. In the tensile specimens, the pores were an order of magnitude smaller than the grains in most specimens, while in the compressive specimens, the grains are slightly smaller than the pores. As reported by Simone and Gibson [1], the grain structure and pore structure have significant influence on the yield strength. Another consideration is that each group of specimens was produced using a different casting apparatus and control parameters. This is important because of the particular sensitivity of copper to processing methods.

For an idealized hexagonal cell honeycomb with low relative density, the out-of-plane plastic collapse stress by plastic buckling of the cell walls is

$$\sigma^*_{pl} = 5.6\ \sigma_{YS}\,(t/l)^{5/3} \quad (4)$$

where σ_{YS} is the yield strength of the solid, t is the cell-wall thickness and l is the cell-edge length [5, 10]. Wierzbicki [10] showed that low relative density metal honeycombs compressed out-of-plane deform linear elastically until the initiation of plastic buckling, after which they typically maintain a roughly constant load resistance until the onset of densification. The compressive stress–strain curves of the GASAR specimens are very different from those produced by Wierzbicki [10] owing to their high relative density and their inconsistent microstructure.

For a honeycomb with hexagonal cells and with a relative density greater than 0.65, the ratio t/l is greater than 0.30, which causes the plastic collapse stress computed by Equation 4 to exceed significantly the stress at which uniaxial yielding of the cell walls initiates, which is given by

$$\sigma^*_Y = \left(\frac{\rho^*}{\rho_s}\right)\sigma_{YS} \quad (5)$$

This implies that the solid material in the cell walls will yield at a stress lower than that required to initiate cell-wall buckling. For the GASAR specimens, this was confirmed through examination of the deformation of specimens compressed to 10% strain and 30% strain. While significant localized cell-wall buckling was observed in the specimens compressed to 30% strain, as seen in Fig. 4, specimens compressed to 10% strain showed little or no cell-wall buckling. After the initial yielding of the cell walls, the load resistance of the specimen increases due to the strain hardening of the solid copper in the cell walls. Cell walls will begin to buckle locally only after the load resistance has increased sufficiently. The strain hardening of the solid cell-wall material therefore causes a progressive increase in the load resistance after the initial yielding.

Because the microstructure of the GASAR specimens, as seen in Fig. 1, is highly non-uniform, the resistance of the cell walls to plastic buckling is also non-uniform. As the load resistance increases due to strain hardening, localized buckling of the cell walls initiates in the plane of lowest resistance to cell-wall buckling, and progresses to regions of higher resistance only as the applied stress increases. The densification of the specimens is similarly progressive, with certain regions densifying at a significantly lower applied stress than others. At higher strains, the increase in load resistance is due to the dilation of the cross-sectional area of the solid as well as strain hardening.

The combined effect of the high relative density of the GASAR materials and their non-uniform microstructure causes the strain-hardening effect after yielding and the gradual transition from plastic collapse to densification exhibited by the stress–strain curves shown in Fig. 3. The influence of these effects is strongest with the higher relative density specimens because both the non-uniformity of the specimen microstructure and the difference between the buckling stress and yield stress increase with relative density. As the relative density increases, the stress–strain behaviour approaches that of a solid ingot, and as relative density decreases, the stress–strain behaviour approaches that described by Wierzbicki [10].

The cell walls of low relative density honeycomb structures typically buckle with a wavelength comparable to the cell-edge length [5, 10]. The porous GASAR copper exhibits a buckling wavelength significantly longer than the cell-edge length. The increase in the buckling wavelength is due to the high thickness to length ratio (t/l) of the cell walls and the decreased lateral restraint caused by the low specimen size to pore size ratio. The linear decrease in densification strain with increasing relative density is consistent with established out-of-plane honeycomb behaviour [5].

5. Conclusion

The pore and grain structure of the porous GASAR specimens were found to be highly variable. In general, the aspect ratio of the pores and the grains increased with decreasing relative density. The grain diameter was found to be 60%–70% of the pore diameter, whereas in porous GASAR copper with microscopic pores, the grains were significantly larger than the pores [1].

The Young's modulus and compressive yield strength of the porous copper increase linearly with increasing relative density, while the densification strain decreases linearly. The compressive yield strengths were significantly lower than previously measured values in tension [1].

The porous GASAR copper exhibited significant strain hardening after initial yielding. This was due to the fact that the plastic buckling stress is significantly higher than the yield stress for high relative density honeycombs tested out-of-plane. As would be expected, the strain hardening was most evident in the higher relative density specimens. Plastic buckling and densification were found to occur progressively due to non-uniformity of the microstructure of the specimens.

Acknowledgement

The authors are grateful for the financial support of the Office of Naval Research (Contract N00014-93-1-1330).

References

1. A. E. SIMONE and L. J. GIBSON, *Acta Metall. Mater.* (1995) **44** (4) (1996) 1437.
2. "Annual Book of ASTM Standards", Vol. 3.01 Test Method E9 (American Society for Testing and Materials, Philadelphia, PA, 1995).
3. *Idem*, Test Method E340 (American Society of Testing and Materials, Philadelphia, PA, 1995).
4. *Idem*, Test Method E407 (American Society of Testing and Materials, Philadelphia, PA, 1995).
5. L. J. GIBSON and M. F. ASHBY, "Cellular Solids: Structure and Properties" (Pergamon Press, Oxford, 1988).
6. W. F. HOSFORD and W. A. BACKOFEN, in "Proceedings, Ninth Sagamore Army Materials Conference: Fundamentals of Deformation Processing", (Syracuse University, Syracuse, NY, 1964) pp. 259–293.
7. American Society of Metals Metals Handbook, Vol. 2 "Properties and Selection: Nonferrous Alloys and Pure Metals", 9th Edn. (American Society of Metals, Metals Park, OH, 1979).
8. J. WEERTZ, *Z. Metallkde* **5** (1933) 25.
9. J. H. LAFLEN, *J. Eng. Mater. Technol.* **105** (1983) 307.
10. T. WIERZBICKI, *Int. J. Impact Eng.* **1** (2) (1983) 157.

Received 8 January
and accepted 18 March 1996